Energy-Efficient Network Selection with Mobility Pattern Awareness in An Integrated WiMAX and WiFi Network

Wen-Hsin Yang, You-Chiun Wang, Yu-Chee Tseng, and Bao-Shuh P. Lin

Abstract—To provide wireless Internet access, WiFi networks have been deployed in many regions such as buildings and campuses. However, WiFi networks are still insufficient to support ubiquitous wireless service due to their narrow coverage. One possibility to resolve this deficiency is to integrate WiFi networks with the wide-range WiMAX networks. Under such an integrated WiMAX and WiFi network, how to conduct energy-efficient handovers is a critical issue. In this paper, we propose a *handover scheme with geographic mobility awareness (HGMA)*, which considers the historical handover patterns of mobile devices. HGMA can conserve the energy of handovering devices from three aspects. Firstly, it prevents mobile devices from triggering unnecessary handovers according to their received signal strength and moving speeds. Secondly, it contains a *handover candidate selection (HCS) method* for mobile devices to intelligently select a subset of WiFi access points or WiMAX relay stations to be scanned. Therefore, mobile devices can reduce their network scanning and thus save their energy. Thirdly, HGMA prefers mobile devices staying in their original WiMAX or WiFi networks. This can prevent mobile devices from consuming too much energy on interface switching. In addition, HGMA prefers the low-tier WiFi network over the WiMAX network and guarantees the bandwidth requirements of handovering devices. Simulation results show that HGMA can save about 59% to 80% of energy consumption of a handover operation, make mobile devices to associate with WiFi networks with 16% to 62% more probabilities, and increase about 20% to 61% of QoS satisfaction ratio to handovering devices.

Index Terms—energy efficiency, handover, network selection, WiFi, WiMAX, wireless network.

1 Introduction

Broadband network applications, such as video streaming and VoIP, have recently become popular and have been embraced by many handheld devices. Meanwhile, in many buildings and campuses, WiFi networks have been densely deployed. However, service regions of WiFi networks are still limited due to WiFi's narrow coverage range. To support seamless wireless access, we propose integrating WiFi networks with the emerging WiMAX networks, which are known to have a theoretical data rate of up to 75 Mbps and a transmission range of up to 50 km [1], [2]. WiMAX is considered as a potential candidate to support global broadband services. In this paper, we consider an integrated WiMAX and WiFi network, as shown in Fig. 1. The WiMAX network serves as a wireless backbone with relay capability and each WiFi *access point (AP)* is connected to a WiMAX *relay station (RS)*. Each *mobile device (MD)* is equipped with dual WiMAX and WiFi interfaces to access both networks, but it will only keep one interface active at a time to save energy.

Under this integrated WiMAX and WiFi network, how to conduct energy-efficient handovers for battery-powered MDs is a critical issue. Since WiFi networks are often deployed to cover certain indoor and outdoor regions (e.g., rooms and campuses), users' mobility is likely to follow some geographic patterns. Therefore, MDs would also handover in some predictable ways, which we call it as the *geographic mobility (GM) feature* of MDs. References [3]–[5] indicate that the GM feature has a significant effect on designing handover schemes. Actually, properly exploiting the GM feature can help conserve MDs' energy due to handover. In this paper, we propose a *handover scheme with geographic mobility awareness (HGMA)*, which can conserve MDs' energy from three aspects. Firstly, it prevents MDs from conducting too frequent handovers in a short duration (called *ping-pong effect*). HGMA will measure the moving speeds and *received signal strength (RSS)* of MDs to avoid unnecessary handovers. Secondly, we develop a *handover candidate selection (HCS) method* for MDs to intelligently select a subset of WiFi APs or WiMAX RSs to be scanned, according to MDs' GM features. Thirdly, HGMA prefers MDs staying in their original WiMAX or WiFi networks. This can save MDs' energy by preventing them from switching network interfaces too frequently.

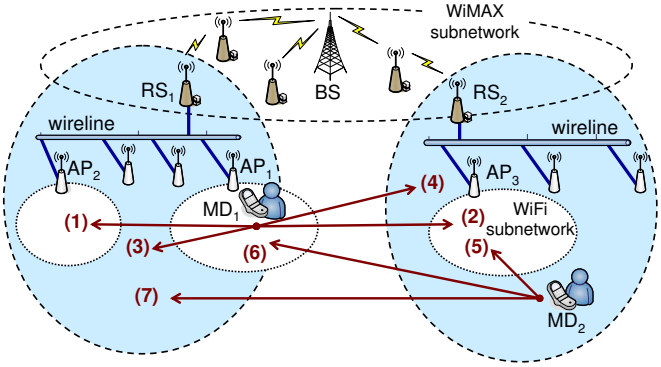

Fig. 1: An integrated WiMAX and WiFi network.

In the literature, research efforts [6]–[10] have focused on how to conduct handovers between a low-bandwidth cellular

W.-H. Yang, Y.-C. Wang, and Y.-C. Tseng are with the Department of Computer Science, National Chiao-Tung University, Hsin-Chu, 30010, Taiwan.
E-mail: {wenhsin, wangyc, yctseng}@cs.nctu.edu.tw
B.-S. P. Lin is with the Information and Communications Research Laboratories, Industrial Technology Research Institute, Chutung, Hsinchu, 31040, Taiwan.
E-mail: bplin@itri.org.tw

network and high-bandwidth WLANs. They focus on making handover decisions to obtain a higher bandwidth for MDs, so the results may not be directly applied in our integrated WiMAX and WiFi network because both WiMAX and WiFi are high-bandwidth networks. The work [11] proposes a proactive handover scheme between WLANs and a 3G network. It maintains a handover trigger table that records the locations where APs' signals will drop significantly. This work requires the knowledge of MDs' positions to decide whether it should trigger pre-handoff operations. The handover issue in a heterogeneous wireless network has been widely discussed in [12]–[23] by favoring networks with wide coverage. Nevertheless, our handover scheme prefers keeping MDs in their original networks to avoid too frequent interface switching.

Several studies consider the handover issue in an integrated WiMAX and WiFi network. The work [24] avoids unnecessary handovers in an integrated IEEE 802.16a and IEEE 802.11n network by detecting the changes of RSS. It prefers keeping MDs in the IEEE 802.11n network to get a higher bandwidth. Reference [25] proposes a bandwidth-based fuzzy handover scheme in an integrated IEEE 802.16 and IEEE 802.11 network. Reference [26] proposes a general architecture to integrate IEEE 802.11 and IEEE 802.16 networks under the IEEE 802.21 *media independent handover (MIH)* framework to manage the handover procedure. The work [27] combines SIP (session initial protocol) and MIH to manage the handovers between IEEE 802.11e and IEEE 802.16 networks, where SIP is to handle the end-to-end QoS requirements of multimedia sessions. Reference [28] considers using the MIH framework to manage handovers in WiMAX and WiFi networks. The work in [29] adopts MIH to support always-on connectivity services with QoS provision of MDs in integrated WiMAX and WiFi networks. Reference [30] proposes an analytical model based on the economical facet to unravel the handover design tradeoffs between maximizing the service provider profit and satisfying the MDs' performance requirements in hierarchical WiMAX-WiFi networks. As can be seen, these work do not consider the energy issue of MDs. The work [31] considers that WiMAX *base stations (BSs)* will periodically broadcast the density of WiFi APs within their coverage to help MDs to adjust their active scan interval to search for APs. This can help reduce MDs' energy consumption, but it differs from our work because we focus on reducing scans in both directions and BSs do not need to conduct such broadcasts. The work [32] proposes a *vertical handoff translation center (VHTC)* architecture to improve transmission QoS of MDs. While [32] considers a centralized solution, our HGMA scheme is a distributed one because each AP and RS will help MDs decide their handover targets. Besides, VHTC does not consider the energy issue of MDs. In [33], an architecture of *WiMAX/WiFi access point (W^2-AP)* devices is proposed to combine the WiMAX and WiFi technologies. The protocol operation of the WiFi hotspots is the same as that of the WiMAX network, so W^2-AP devices can support connection-oriented transmissions and QoS in a similar fashion to the WiMAX network. However, it is not compatible to existing WiFi networks.

The major contributions of this paper are three-fold. Firstly, we identify the GM feature of MDs in an integrated WiMAX and WiFi network. Secondly, we propose an energy-efficient HGMA handover scheme by adopting the GM feature. Our HGMA scheme can eliminate unnecessary handovers, reduce the number of network scanning, and avoid switching network interfaces too frequently. Extensive simulation results show that HGMA can conserve about 59% to 80% energy consumption to conduct a handover operation, save about 70% of network scanning, and reduce about 31% of interface switching. Thirdly, HGMA prefers the low-tier WiFi network over the WiMAX network, and guarantees the bandwidth requirements of handovering MDs. It is verified by simulations that HGMA can make MDs to associate with WiFi networks with 16% to 62% more probabilities, and increase 20% to 61% of possibility that WiFi APs can afford the demanded bandwidths of MDs after they handover to.

The rest of this paper is organized as follows. Section 2 presents our system architecture. Section 3 proposes our handover schemes. Simulation results are given in Section 4. Section 5 concludes this paper.

2 The Integrated WiMAX and WiFi Network Architecture

The system architecture of our integrated WiMAX and WiFi network has two tiers, as shown in Fig. 1. The upper tier is a WiMAX network where each BS is connected to multiple RSs. The lower tier is WiFi networks with lots of APs connected to RSs and then to BSs. We say that an RS and an AP have a *parent-child relationship* if they are connected through a wireline. The wireless coverage of adjacent APs are not necessarily always continuous. We assume that the whole service area is completely covered by the WiMAX network, but may not be completely covered by the WiFi networks, in which both WiMAX and WiFi networks belong to the same service provider. Each MD is equipped with dual 802.11b/g and 802.16e interfaces. However, it tends to keep one interface active at once.

There are seven handover cases in the integrated WiMAX and WiFi network, as numbered by 1–7 in Fig. 1:

1) MD_1 handovers from AP_1 to AP_2. AP_1 and AP_2 have the same parent RS_1.
2) MD_1 handovers from AP_1 to AP_3. AP_1 and AP_3 have different parent RSs.
3) MD_1 handovers from AP_1 to its parent RS_1.
4) MD_1 handovers from AP_1 to another RS_2.
5) MD_2 handovers from RS_2 to its child AP_3.
6) MD_2 handovers from RS_2 to another AP_1.
7) MD_2 handovers from RS_2 to RS_1.

In cases 3 and 4, the MD has to switch to the WiMAX mode. In cases 5 and 6, the MD can switch to the WiFi mode to enjoy a higher bandwidth. The above cases can be categorized into two classes. The HO_{AP} *class* contains handover cases 1–4, where an MD moves out of its current AP. The HO_{RS} *class* contains handover cases 5–7, where an MD moves out of its current RS.

Our goal is to design a handover strategy to minimize the energy consumption of MDs such that the ping-pong effect can be alleviated, the number of network scanning can be minimized, the frequency of interface switching can be reduced, and the possibility that MDs associate with APs can be increased. Table 1 summarizes our notations.

3 The HGMA Scheme

Fig. 2 shows the flowchart of our HGMA scheme. It has two parts, namely $\mathrm{HO_{AP}}$ and $\mathrm{HO_{RS}}$ classes.

TABLE 1: Summary of notations.

notations	definition
e_{MD}	energy level of an MD (0 to γ, empty to fully-charged)
$\varepsilon_{\mathrm{RS}}$	energy threshold to switch to the WiFi interface in the $\mathrm{HO}_{\mathrm{RS}}$ class
V	current speed of an MD
B_{MD}	bandwidth demand of an MD
Δ_{MD}	dwell-time of an MD
$V_0(AP)/V_0(RS)$	average speed of an MD when it is within a WiFi/WiMAX network
$T_{AP}(V)/T_{RS}(V)$	average observation period for an MD to measure RSS in a WiFi/WiMAX network
$S_{AP}^{\min}/S_{RS}^{\min}$	minimum RSS threshold to trigger a handover in the $\mathrm{HO}_{\mathrm{AP}}/\mathrm{HO}_{\mathrm{RS}}$ class
S_{AP}/S_{RS}	RSS threshold to check if trigger a handover in the $\mathrm{HO}_{\mathrm{AP}}/\mathrm{HO}_{\mathrm{RS}}$ class
n_{exp}	expected number of candidate APs/RSs
$\mathcal{L}_{\mathrm{AP}}(RS_i)$	table in an MD that records the neighboring APs of the associating RS_i
$\mathcal{C}_{\mathrm{AP}}/\mathcal{C}_{\mathrm{RS}}$	candidate APs/RSs returned by HCS
$\mathcal{T}_{\mathrm{AP}}(A_i)/\mathcal{T}_{\mathrm{RS}}(A_i)$	table that records neighboring APs/RSs of an AP A_i
$\mathcal{T}_{\mathrm{AP}}(R_i)/\mathcal{T}_{\mathrm{RS}}(R_i)$	table that records neighboring APs/RSs of an RS R_i

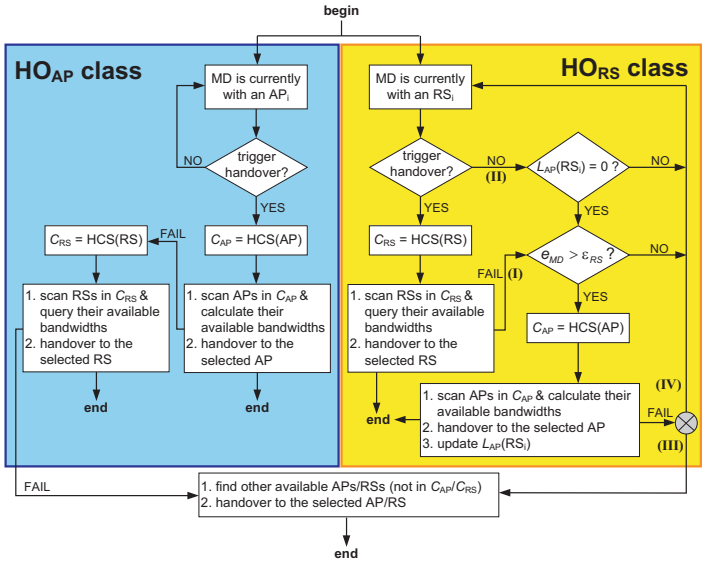

Fig. 2: The HGMA scheme.

$\mathrm{HO}_{\mathrm{AP}}$ class: When an MD is currently associated with an AP_i, it periodically checks whether it should trigger a handover. The checking procedure will be discussed in Section 3.1. If triggering a handover is needed, it will invoke the HCS method in Section 3.2 to select a set of candidate APs, called $\mathcal{C}_{\mathrm{AP}}$. The MD then scans those APs in $\mathcal{C}_{\mathrm{AP}}$ and calculates each AP's available bandwidth (for example, the results in [34], [35] point out some ways to calculate an AP's remaining bandwidth). Then, among those APs whose available bandwidths can afford the MD's traffic demand B_{MD}, the MD will select the AP with the strongest RSS to handover to. However, if the MD fails to find an available AP in $\mathcal{C}_{\mathrm{AP}}$, it will invoke the HCS method, which will return a set of candidate RSs, call $\mathcal{C}_{\mathrm{RS}}$. Then, it scans these RSs and queries their available bandwidths by a request-grant protocol. Among those RSs whose available bandwidths can afford the bandwidth demand B_{MD}, the MD will select the RS with the strongest RSS to handover to. However, if no feasible RS can be found, the MD will search for other APs/RSs (not in $\mathcal{C}_{\mathrm{AP}}/\mathcal{C}_{\mathrm{RS}}$).

$\mathrm{HO}_{\mathrm{RS}}$ class: When an MD is currently associated with an RS_i, it also periodically checks whether it should trigger a handover. If needed, the MD will invoke the HCS method and then scan the candidate RSs in $\mathcal{C}_{\mathrm{RS}}$. If this step fails (case I in Fig. 2), it will check whether its current energy level e_{MD} is larger than a predefined threshold $\varepsilon_{\mathrm{RS}}$. If so, the MD will invoke the HCS method, turn on its WiFi interface, scan the candidate APs in $\mathcal{C}_{\mathrm{AP}}$, find one target AP, and add the selected AP into its $\mathcal{L}_{\mathrm{AP}}(RS_i)$, where $\mathcal{L}_{\mathrm{AP}}(RS_i)$ is a table that records all APs to which the MD has ever handovered from its current RS_i. In the above discussion, even if the MD decides not to trigger handover (see case II in Fig. 2), it will still try to search for APs if both $\mathcal{L}_{\mathrm{AP}}(RS_i) \neq \emptyset$ (i.e., there are potential APs in this RS_i's neighborhood) and $e_{\mathrm{MD}} > \varepsilon_{\mathrm{RS}}$ (i.e., the MD has sufficient energy to conduct extra network scanning). In this case, the MD will invoke the HCS method, scan the candidate APs in $\mathcal{C}_{\mathrm{AP}}$, find one target AP, and add the selected AP into its $\mathcal{L}_{\mathrm{AP}}(RS_i)$. However, when the MD cannot find any feasible RS/AP, two cases will happen (refer to the switch point '$\otimes$' in Fig. 2). If the MD arrives at $\otimes$ from case I, it will follow case III and search for other APs/RSs not in $\mathcal{C}_{\mathrm{AP}}/\mathcal{C}_{\mathrm{RS}}$. However, if the MD arrives at $\otimes$ from case II, it will follow case IV and keep associating with its current RS. We remark that one possible way to define $\varepsilon_{\mathrm{RS}}$ is to set it as a fixed value such as $\lfloor \frac{\gamma}{2} \rfloor$, where $\gamma \in \mathbb{N}$ is the maximum energy level of an MD when it is fully-charged. Another way is to adaptively change $\varepsilon_{\mathrm{RS}}$ according to the MD's current speed V. For example, let $V_0(RS)$ be the average speed of the MD when it is within WiMAX networks. We can update $\varepsilon_{\mathrm{RS}} = \min\{1, \frac{V}{V_0(RS)}\} \times \varepsilon_{RS}^{D}$, where ε_{RS}^{D} is the default value of $\varepsilon_{\mathrm{RS}}$. Specifically, when $V < V_0(RS)$, a smaller $\varepsilon_{\mathrm{RS}}$ is set since the MD has more opportunity to stay in its originally serving RS. In this case, we can encourage the MD to search for neighboring APs to handover to.

To summarize, our HGMA scheme has several special designs to conserve MDs' energy. Firstly, to prevent MDs from conducting unnecessary handovers due to the ping-pong effect, we propose a handover-triggering process in Section 3.1, which is based on the RSSs and moving speeds of MDs. Secondly, to reduce the number of network scanning, we design the HCS method in Section 3.2, which is based on the GM feature of MDs to select only a subset of neighboring APs/RSs to be scanned. Thirdly, to reduce the frequency of interface switching, we make an MD in the $\mathrm{HO}_{\mathrm{AP}}$ class to scan available APs first, and then scan RSs when no AP can be found. The similar design is also applied to the $\mathrm{HO}_{\mathrm{RS}}$ class. Last, to increase the probability that MDs stay in WiFi networks, we search for APs first in the $\mathrm{HO}_{\mathrm{AP}}$ class when a handover event is triggered. Also, in the $\mathrm{HO}_{\mathrm{RS}}$ class, an MD can still try to search for APs if its energy level is sufficient.

3.1 When to Trigger a Handover

The process to trigger a handover event is shown in Fig. 3. Here, we assume that an MD can measure its current speed V. In the $\mathrm{HO}_{\mathrm{AP}}$ class (refer to Fig. 3(a)), an MD will periodically

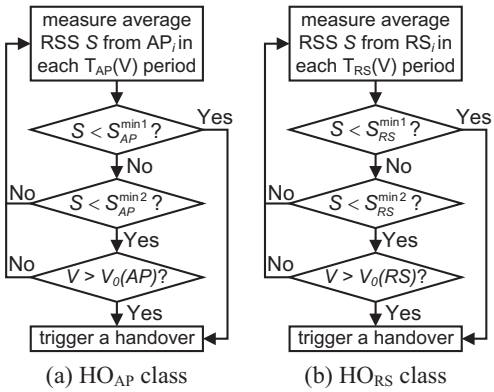

(a) $\mathrm{HO_{AP}}$ class (b) $\mathrm{HO_{RS}}$ class

Fig. 3: Checking procedures to trigger a handover event.

measure the average RSS S from its associating AP_i. Typically, a lower RSS will trigger an MD to start a handover process. However, to alleviate the ping-pong effect when an MD is around cell boundaries due to temporal RSS dropping, we propose adaptively adjusting an *observation interval* as follows:

$$T_{AP}(V) = \frac{V_0(AP)}{V} \times T_0(AP),$$

where $V_0(AP)$ is the average speed of the MD when it is within WiFi networks and $T_0(AP)$ is a constant representing the MD's average observation interval. If its average RSS is continuously below the handover threshold $S_{AP}^{\min 1}$ over the interval $T_{AP}(V)$, it means that the MD is very close to the coverage boundary of that AP and thus the MD should trigger a handover event. Otherwise, we check whether S is continuously below a second threshold $S_{AP}^{\min 2}$, where $S_{AP}^{\min 2} > S_{AP}^{\min 1}$. If so, it means that the MD is *near* the coverage boundary of AP_i and we will further check whether the MD's current speed $V > V_0(AP)$. If the speed criterion is met, the MD will also trigger a handover event because it is likely to move out of its current AP_i.

Similarly, in the $\mathrm{HO_{RS}}$ class (refer to Fig. 3(b)), an MD will continuously measure the average RSS from its associating RS_j for an observation interval:

$$T_{RS}(V) = \frac{V_0(RS)}{V} \times T_0(RS),$$

where $T_0(RS)$ is the average observation interval to measure RSS in the WiMAX network. When the RSS S is continuously below the minimum threshold $S_{RS}^{\min 1}$, a handover event should be triggered. Otherwise, if both $S < S_{RS}^{\min 2}$ and $V > V_0(RS)$, the MD should also trigger a handover event, where $S_{RS}^{\min 2} > S_{RS}^{\min 1}$ is a secondary threshold.

3.2 The HCS Method

HCS exploits the GM feature based on past handover patterns of MDs to select candidate APs/RSs to be scanned. Specifically, for each AP A_i, we maintain two tables $\mathcal{T}_{\mathrm{AP}}(A_i)$ and $\mathcal{T}_{\mathrm{RS}}(A_i)$ to record the information of A_i's neighboring APs and RSs, respectively. An AP A_j is in A_i's $\mathcal{T}_{\mathrm{AP}}(A_i)$ if A_i and A_j share the same parent RS or an MD has ever handovered from A_i to A_j. An RS is in A_i's $\mathcal{T}_{\mathrm{RS}}(A_i)$ if it is A_i's parent RS or an MD has ever handovered from A_i to this RS. Similarly, for each RS R_i, we maintain its neighboring RSs and APs in tables $\mathcal{T}_{\mathrm{RS}}(R_i)$ and $\mathcal{T}_{\mathrm{AP}}(R_i)$, respectively. An RS R_j is in R_i's $\mathcal{T}_{\mathrm{RS}}(R_i)$ if an MD has ever handovered from R_i to R_j. An AP is in R_i's $\mathcal{T}_{\mathrm{AP}}(R_i)$ if it is a child AP of R_i or an MD has ever handovered from R_i to this AP.

In the above four tables, three extra pieces of information are maintained. Without loss of generality, we consider table $\mathcal{T}_{\mathrm{AP}}(A_i)$ of an AP A_i. For each A_j in $\mathcal{T}_{\mathrm{AP}}(A_i)$, we record three statistics over a time interval: $v(A_i, A_j)$ counts the total number of MDs that have ever handovered from A_i to A_j, $t(A_i, A_j)$ records the average dwell-time in A_i for these MDs, and $b(A_i, A_j)$ is the average available bandwidth provided by A_j when these MDs handovered from A_i. The other three tables $\mathcal{T}_{\mathrm{RS}}(A_i)$, $\mathcal{T}_{\mathrm{AP}}(R_i)$, and $\mathcal{T}_{\mathrm{RS}}(R_i)$ also maintain the similar information.

HCS works as follows. Without loss of generality, we consider an MD that is currently associated with AP A_i and intends to scan other APs. HCS will select a number $n = \min\{n_{\exp}, |\mathcal{T}_{\mathrm{AP}}(A_i)|\}$ of candidate APs from its $\mathcal{T}_{\mathrm{AP}}(A_i)$ to be scanned, where $n_{\exp}$ is the expected number of candidate APs and $|\mathcal{T}_{\mathrm{AP}}(A_i)|$ is the total number of APs in $\mathcal{T}_{\mathrm{AP}}(A_i)$. One way to define $n_{\exp}$ is to consider the MD's remaining energy. When the MD has more energy, a larger $n_{\exp}$ can be used. For example, supposing that the MD remains l percent of energy, we can set its $n_{\exp} = \lfloor l \times \gamma \rfloor$. To select these n APs, we calculate the *similarity* $s(A_i, A_j)$ of A_i and A_j for each $A_j \in \mathcal{T}_{\mathrm{AP}}(A_i)$ as follows:

$$\sqrt{W_v \times f_v(A_i, A_j)^2 + W_t \times f_t(A_i, A_j)^2 + W_b \times f_b(A_i, A_j)^2}, \quad (1)$$

where W_v, W_t, and W_b are weights such that $W_v + W_t + W_b = 1$ and

$$f_v(A_i, A_j) = \frac{v(A_i, A_j)}{\sum_{A_k \in \mathcal{T}_{\mathrm{AP}}(A_i)} v(A_i, A_k)}, \quad (2)$$

$$f_t(A_i, A_j) = \frac{\min\{\Delta_{\mathrm{MD}}, t(A_i, A_j)\}}{\max\{\Delta_{\mathrm{MD}}, t(A_i, A_j)\}}, \quad (3)$$

$$f_b(A_i, A_j) = \min\left\{1, \frac{b(A_i, A_j)}{B_{\mathrm{MD}}}\right\}, \quad (4)$$

where Δ_{MD} is the current dwell-time that the MD has stayed in A_i and B_{MD} is the MD's bandwidth demand. Then, HCS selects the first n most similar APs in $\mathcal{T}_{\mathrm{AP}}(A_i)$ and stores them in $\mathcal{C}_{\mathrm{AP}}$.

Eq. (1) is to measure the similarity between A_i and A_j. Eqs. (2)–(4) are three factors to be considered and their values should be bounded by $0 \leq f_v(A_i, A_j), f_t(A_i, A_j), f_b(A_i, A_j) \leq 1$. Eq. (2) represents the *visiting frequency* $f_v(A_i, A_j)$ from A_i to A_j in the past handover statistics. Eq. (3) represents the *dwell-time relationship* $f_t(A_i, A_j)$. Recall that $t(A_i, A_j)$ is the average dwell-time before handovering. When the MD's dwell-time Δ_{MD} is closer to $t(A_i, A_j)$, there is a higher probability that the MD will take a handover. Eq. (4) represents the *expected available bandwidth* $f_b(A_i, A_j)$ of A_j. Since $b(A_i, A_j)$ records the past available bandwidth of A_j, we thus prefer those with a larger available bandwidth. However, this value is upper bounded by 1. These factors are given weights W_v, W_t, and W_b. To determine their values, we can consider the moving speed of an MD. For example, we can set

$$W_v = \begin{cases} \frac{V}{V+V_0(AP)} & \text{in } \mathrm{HO_{AP}} \text{ class} \\ \frac{V}{V+V_0(RS)} & \text{in } \mathrm{HO_{RS}} \text{ class,} \end{cases}$$

$$W_t = W_b = \begin{cases} \frac{V_0(AP)}{2\times[V+V_0(AP)]} & \text{in } \mathrm{HO_{AP}} \text{ class} \\ \frac{V_0(RS)}{2\times[V+V_0(RS)]} & \text{in } \mathrm{HO_{RS}} \text{ class.} \end{cases}$$

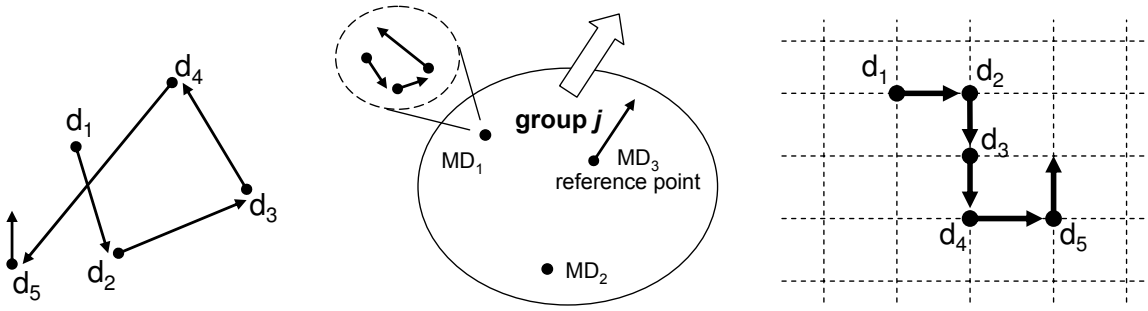

(a) random waypoint (b) reference point group mobility (c) Manhattan grid

Fig. 4: Scenarios of three mobility models.

4 Experimental Results

In this section, we present extensive simulation results to verify the effectiveness of the proposed HGMA scheme. Our simulations are conducted by the IEEE 802.16 modules based on ns-2 [36]. The physical layer adopts an OFDM (orthogonal frequency division multiplexing) module and the radio propagation model is set to two-ray ground. We consider two types of network topologies. In the *dense* topology, each RS has 10 child APs. In the *random* topology, each RS has arbitrarily 0 to 10 child APs. Each MD will consume 5% of its energy every five minutes. We rank an MD's remaining energy by levels. When fully charged, its energy level is γ, where $\gamma \in \mathbb{N}$. The calculation of energy level is as follows:

$$\left\lfloor \frac{\text{current remaining energy}}{\text{fully-charged energy}} \times \gamma \right\rfloor .$$

We set $\varepsilon_{\mathrm{RS}} = 1$ and $W_v = W_t = W_b = \frac{1}{3}$.

The BonnMotion tool [37] is adopted to generate three types of mobility models for MDs. In the *random waypoint (WAYPOINT) model*, as shown in Fig. 4(a), an MD randomly chooses one destination (e.g., d_2) to move to, with an average speed of $[0, 1]\,\mathrm{m/s}$. After reaching its destination, the MD pauses about 120 seconds and then selects another destination (e.g., d_3) to move to. In the *reference point group mobility (GROUP) model*, each MD belongs to one group and the same group of MDs will move in the same direction and have the same speed. The speed is generated randomly from $[0.5, 1.5]\,\mathrm{m/s}$ and the pause time is upper bounded by 60 seconds. An MD may leave its group and join another group with a probability of 0.01. Fig. 4(b) gives an example, where MD_1, MD_2 and MD_3 belong to the same group j. Although MD_1 wants to move to another destination based on its own moving path (the dotted circle), it adapts its direction by following the indication of group j, which depends on the mobility behavior of the reference point MD_3. Thus, with the same speed and direction, MD_1, MD_2 and MD_3 will move simultaneously. In the *Manhattan grid (GRID) model*, MDs move on a number of horizontal and vertical streets in an urban area. The speeds of MDs range from 0.5 to 1 $\mathrm{m/s}$, with a maximum pause time of 120 seconds. Each MD may change its direction when it reaches an intersection, with a turning probability of 0.5. Fig. 4(c) gives an example, where the MD moves along the path of $d_1 \rightarrow d_2 \rightarrow d_3 \rightarrow d_4 \rightarrow d_5$. In our simulations, we set $V_0(AP) = 0.5\,\mathrm{m/s}$, $V_0(RS) = 1\,\mathrm{m/s}$, and $T_0(AP) = T_0(RS) = 100\,\mu\mathrm{s}$. We mainly compare our HGMA scheme with the traditional handover scheme, where a handovering MD will scan all APs/RSs around it.

4.1 Number of Network Scans

Fig. 5 shows the average number of APs scanned by MDs. Clearly, the average number of APs scanned by MDs in the dense topology is larger than that in the random topology because the former has more APs. The traditional handover scheme will ask MDs to scan all possible APs around them, even though they have lower remaining energy. On the contrary, HGMA allows MDs to scan fewer APs when they have lower energy. In this way, the energy of MDs can be conserved. When comparing these three mobility models, we can observe that HGMA will cause more scans in the WAYPOINT model than those in the GROUP and GRID models when there are more than 45% of remaining energy. This is because the WAYPOINT model has a less regular mobility pattern, causing lower predictability, and a higher n_{exp} value is used. With the GROUP and GRID models, the candidate APs/RSs are more predictable. This result supports that our HGMA scheme is capable of decreasing the number of network scans for MDs if they move in some regular patterns. Note that in the WAYPOINT model, the number of APs scanned by MDs plunges when the remaining energy of MDs is within $[40\%, 35\%]$. This is because less handovers are incurred by MDs in the simulation.

Table 2 summarizes the average reduction of the number of scanned APs by our HGMA scheme. HGMA can reduce about 70% of AP scanning, thereby significantly reducing the energy consumption of MDs. Additionally, HGMA works the best when MDs move in the GRID model, especially in the random topology. This is because the GRID model has the most regular mobility pattern for MDs, making the prediction more accurate. On the other hand, even in the non-regular WAYPOINT model, HGMA can still save about 66% to 67% of the scanning events. This clearly shows the advantages of HGMA.

TABLE 2: Reduction of the number of scanned APs by HGMA.

topology	WAYPOINT	GROUP	GRID	average
dense	66.13%	70.12%	70.80%	68.99%
random	67.12%	70.81%	73.11%	70.31%

4.2 Cumulative Number of Interface Switching

Fig. 6 shows the cumulative number of interface switching of MDs. When MDs have more than 40% of remaining energy, HGMA has almost no effect on interface switching. This is because it encourages those MDs associating with RSs to handover to WiFi networks when they have more energy. However, when MDs remain less energy, HGMA will prevent

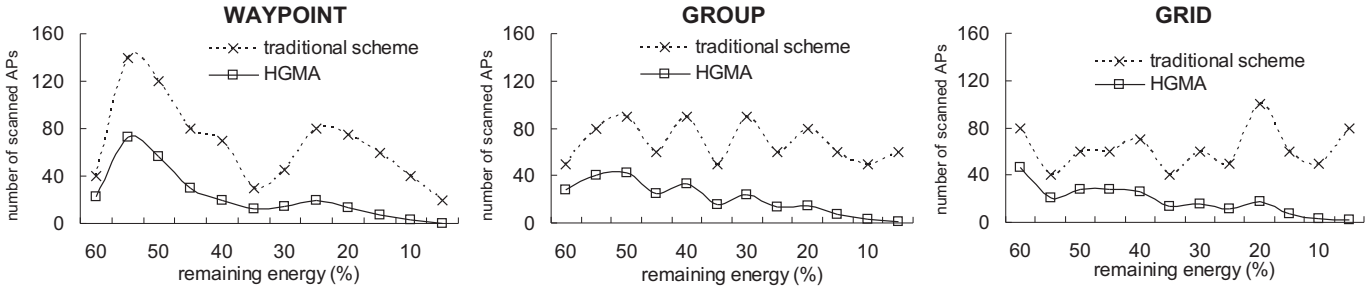

(a) dense topology

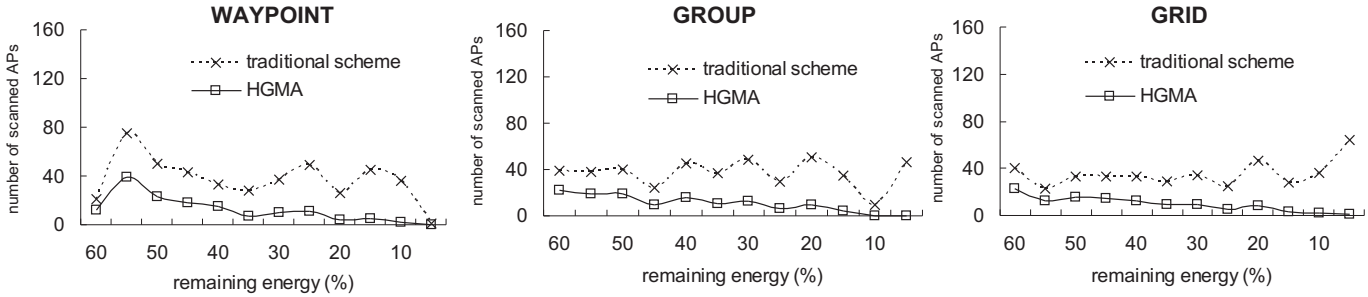

(b) random topology

Fig. 5: Average number of scanned APs in different models.

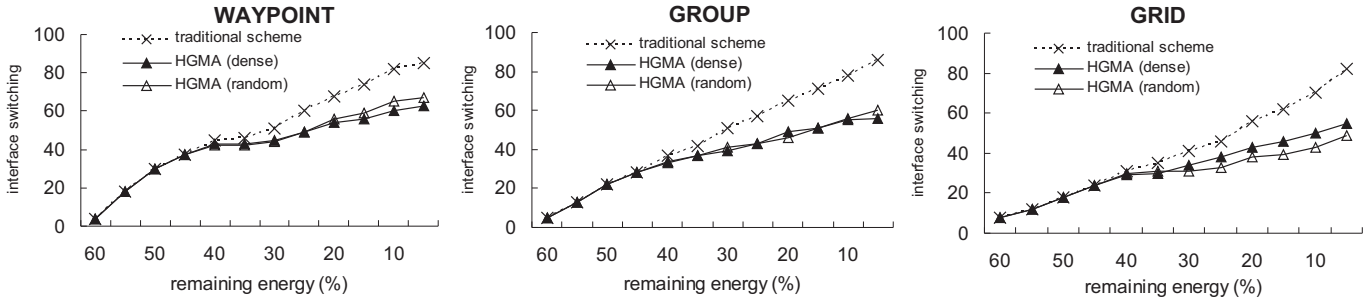

Fig. 6: Cumulative number of interface switching in different models.

them from frequently switching network interfaces to save their energy.

Table 3 summarizes the average reduction of the number of interface switching by HGMA. HGMA can reduce about 31% of interface switching, thus significantly conserving the energy of MDs. In addition, HGMA works better when MDs move in the more regular GROUP and GRID models. On the other hand, even in the non-regular WAYPOINT model, HGMA can still reduce about 21% to 26% of the switching events. This verifies the effectiveness of HGMA.

TABLE 3: Reduction of the number of interface switching by HGMA.

topology	WAYPOINT	GROUP	GRID	average
dense	25.88%	34.88%	32.93%	31.23%
random	21.18%	30.23%	40.24%	30.55%

4.3 Cumulative Number of Handovers to APs

Fig. 7 shows the cumulative number of handovers to APs. When trying to associate with a WiFi AP, we simulate an *association failure probability* $p = 0.2 \sim 0.4$ (this is to take factors such as contention into account). When p increases, the number of handovers to APs will decrease. From Fig. 7(a), we can observe that HGMA can still perform well even with a larger p. This is because the AP density is large enough and thus MDs can easily find an AP to handover to. On the other hand, in Fig. 7(b), the improvement of HGMA is less significant when p is larger. This is because MDs may not always find suitable APs in their neighborhood. However, when MDs move in the more regular GROUP and GRID models, HGMA can increase the possibility that MDs associate with WiFi networks.

Table 4 gives the improvement of the number of handovers to APs by HGMA. In average, HGMA can increase 62% and 16% of probability for MDs to associate with WiFi networks when p is set to 0.2 and 0.4, respectively.

TABLE 4: Improvement of the number of handovers to APs by HGMA.

p	topology	WAYPOINT	GROUP	GRID	average
0.2	dense	1.769	1.673	1.838	1.760
	random	1.477	1.480	1.476	1.478
0.4	dense	1.231	1.203	1.270	1.235
	random	1.068	1.105	1.071	1.081

4.4 Dwell-time in WiFi Networks

Fig. 8 illustrates the average dwell-time that MDs stay in WiFi networks during one hour. When the failure probability p increases, the dwell-time will reduce because MDs may fail in the association more often. When MDs move in a more regular pattern, they can stay in WiFi networks for a longer time when

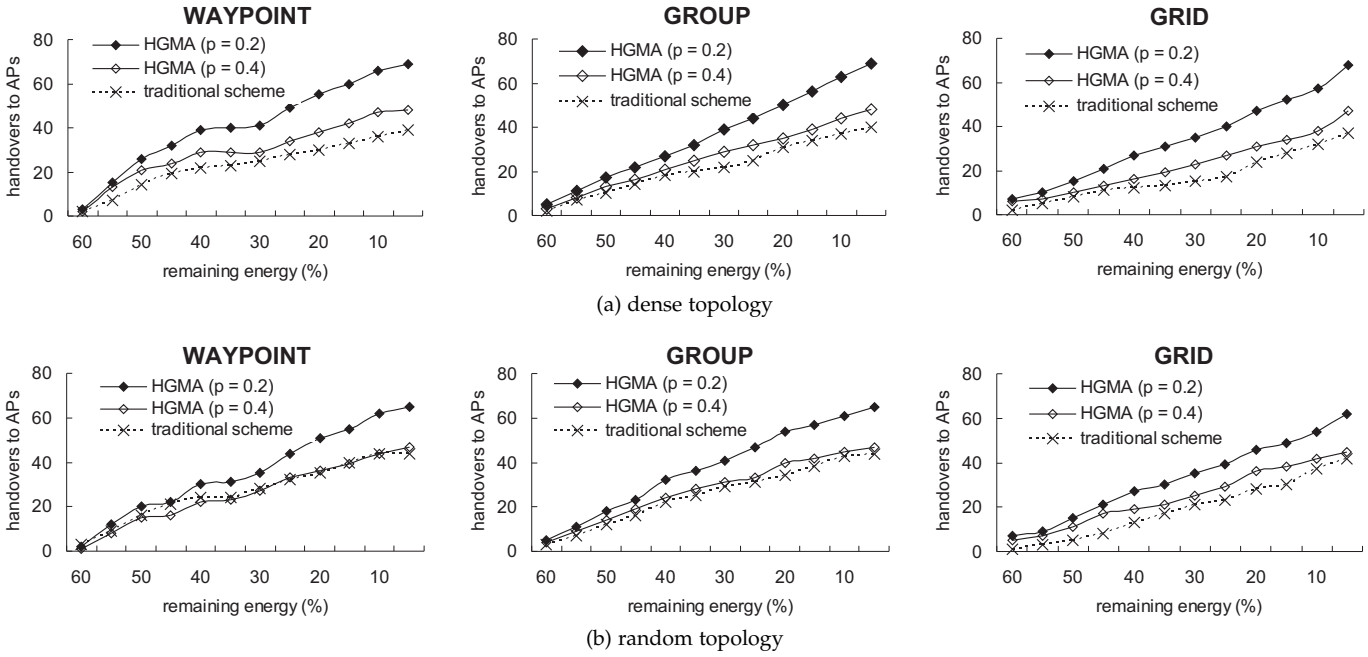

Fig. 7: Cumulative number of handovers to APs in different models.

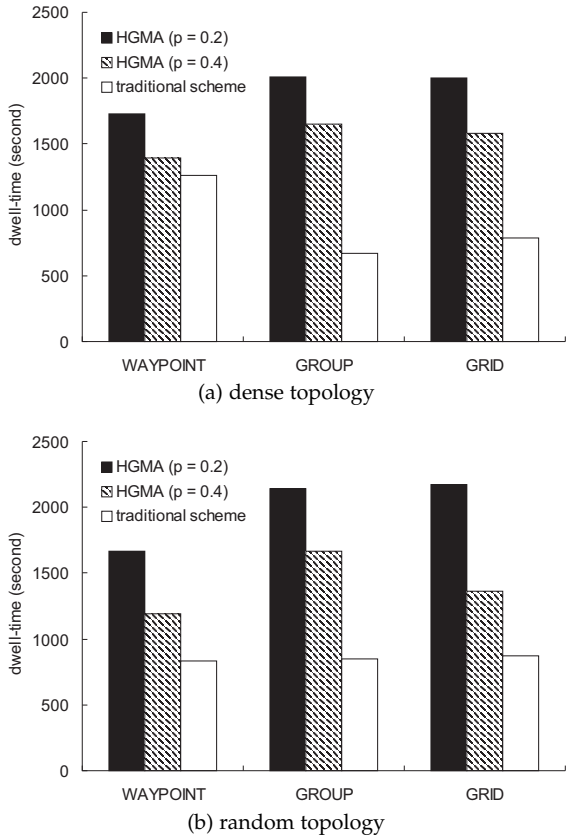

Fig. 8: Average dwell-time of MDs in WiFi networks during one hour in different models.

our HGMA scheme is adopted. From Fig. 8, we can observe that HGMA can keep MDs in WiFi networks more than half an hour in the GROUP and GRID models when $p = 0.2$.

Table 5 gives the improvement on average dwell-time in WiFi networks by HGMA. In average, HGMA can increase 132% and 76% of dwell-time for MDs when the p is set to 0.2 and 0.4, respectively.

TABLE 5: Improvement of dwell-time of MDs in WiFi networks by HGMA.

p	topology	WAYPOINT	GROUP	GRID	average
0.2	dense	1.372	2.990	2.548	2.303
	random	2.002	2.526	2.497	2.342
0.4	dense	1.106	2.458	2.020	1.861
	random	1.430	1.967	1.568	1.655

4.5 Energy Consumption

Next, we compare the energy consumption of MDs by HGMA and by the traditional handover scheme. We set $p = 0 \sim 0.4$ and the energy cost for an MD to scan an AP/RS to 1/1.1 unit of energy. Also, the cost to switch network interface is 1 unit of energy. Fig. 9 shows the average energy consumption of MDs to conduct a handover operation. We can observe that when the traditional handover scheme is adopted, MDs will consume much energy even if they remain less energy. This is due to two reasons. Firstly, the traditional handover scheme will make an MD scan all neighboring APs/RSs to determine its handover target. From Fig. 5, we can observe that the number of scanned APs by the traditional handover scheme is still large even though MDs remain less energy. Secondly, the traditional handover scheme will make MDs frequently switch their network interfaces, no matter how much energy they remain (such effect can be found in Fig. 6). Thus, the energy consumption of MDs to conduct a handover operation by the traditional handover scheme may increase when MDs' energy decreases. On the contrary, our HGMA scheme can make MDs spend less energy when conducting handovers. Again, from Figs. 5 and 6, HGMA will reduce the numbers of AP scanning and interface switching when MDs remain less energy. Thus, the energy consumption of MDs to conduct a handover operation by HGMA decreases when MDs' energy decreases. Such phenomenon is more significant when MDs have no more than 30% of remaining energy. When $p = 0$, the energy consumption of MDs is quite less (especially when the remaining energy is lower than 30%), because MDs can easily find an AP to associate with.

Table 6 summarizes the average reduction of energy con-

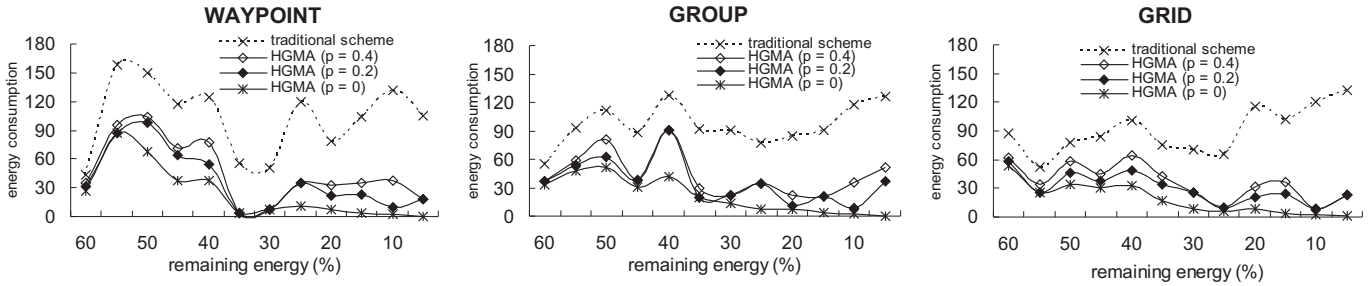

(a) dense topology

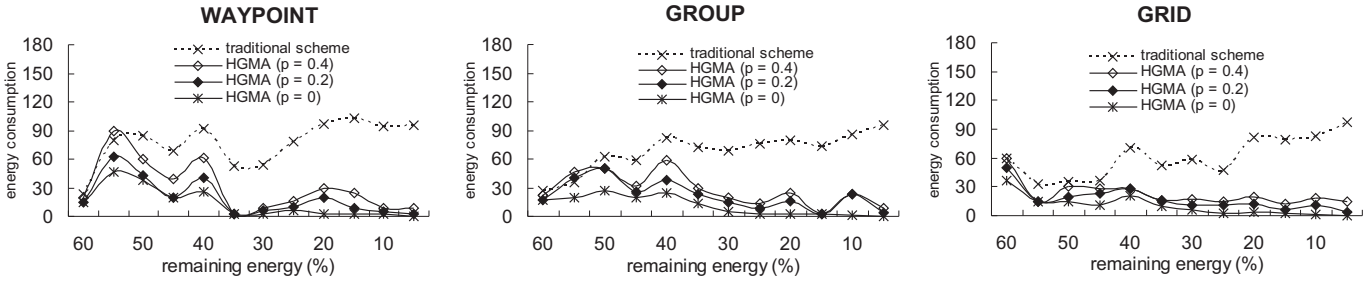

(b) random topology

Fig. 9: Average energy consumption of MDs to conduct a handover operation in different models.

sumption of MDs to conduct a handover operation by HGMA. Clearly. HGMA can reduce the most energy consumption in the GRID model due to MDs' predictable mobility. In average, HGMA can reduce about 80%, 68%, and 59% of energy consumption of handovering MDs when p is set to 0, 0.2, and 0.4, respectively.

TABLE 6: Reduction of energy consumption of MDs to conduct a handover operation by HGMA.

p	topology	WAYPOINT	GROUP	GRID	average
0	dense	76.37%	77.66%	79.17%	77.73%
	random	82.10%	83.50%	83.06%	82.89%
0.2	dense	63.47%	62.34%	66.54%	64.13%
	random	74.40%	67.73%	71.86%	71.33%
0.4	dense	55.48%	54.98%	59.26%	56.57%
	random	60.30%	59.66%	62.57%	60.84%

4.6 QoS Measurement

Last, we measure the *QoS-satisfied handover ratio* by HGMA and by the traditional handover scheme during one hour, which is defined by the ratio of the number of handovers to WiFi networks that can satisfy the demanded bandwidths of handovering MDs to the total number of handovers to WiFi networks. Fig. 10 illustrates the QoS-satisfied handover ratio in different mobility models. We can observe that HGMA outperforms the traditional handover scheme because HCS considers the bandwidth factor (i.e., Eq. (4)) when selecting candidate APs. When p increases, the QoS-satisfied handover ratio of HGMA decreases because MDs may not easily find suitable APs in their neighborhood.

Table 7 shows the improvement of QoS-satisfied handover ratios by HGMA. We can observe that HGMA works better in more regular GROUP and GRID models. In average, HGMA can improve about 61% and 20% of ratio when p is set to 0.2 and 0.4, respectively. This indicates that HGMA can guarantee QoS requirements of handovering MDs.

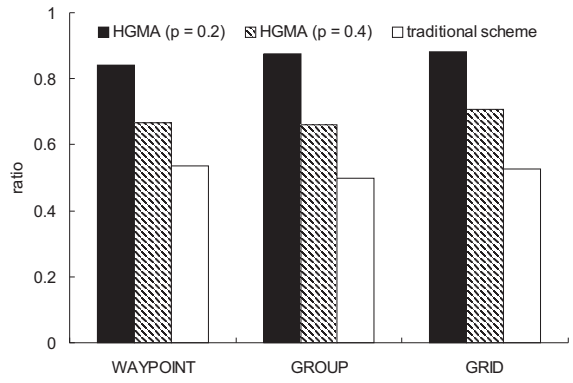

(a) dense topology

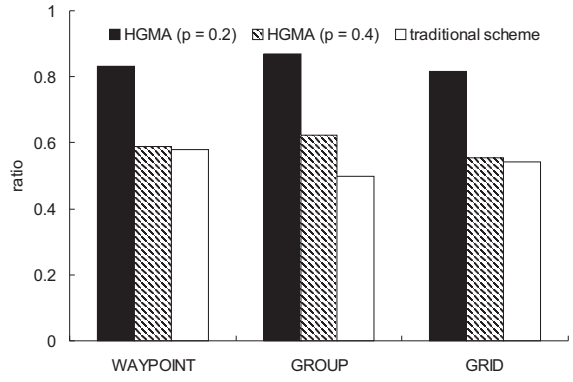

(b) random topology

Fig. 10: QoS-satisfied handover ratios in different models.

TABLE 7: Improvement of QoS-satisfied handover ratios by HGMA.

p	topology	WAYPOINT	GROUP	GRID	average
0.2	dense	1.569	1.75	1.681	1.667
	random	1.435	1.736	1.501	1.557
0.4	dense	1.242	1.321	1.345	1.303
	random	1.017	1.245	1.023	1.095

5 Conclusions

In this paper, we have defined an integrated WiMAX and WiFi network architecture and discussed the corresponding han-

dover scenarios. We have proposed an energy-efficient HGMA scheme that considers the GM feature of MDs. By eliminating unnecessary handovers, reducing the number of network scanning, and avoiding too frequent interface switching, the proposed HGMA scheme can significantly conserve the energy of MDs due to handover. Simulation results have justified the efficiency and improvement of the proposed scheme in various mobility models.

REFERENCES

[1] A. Ghosh, D.R. Wolter, J.G. Andrews, and R. Chen, "Broadband wireless access with WiMAX/802.16: current performance benchmarks and future potential," *IEEE Comm. Magazine*, vol. 43, no. 2, pp. 129–136, 2005.

[2] K. Lu, Y. Qian, H.H. Chen, and S. Fu, "WiMAX networks: from access to service platform," *IEEE Network*, vol. 22, no. 3, pp. 38–45, 2008.

[3] L. Song, D. Kotz, R. Jain, and X. He, "Evaluating next-cell predictors with extensive Wi-Fi mobility data," *IEEE Trans. Mobile Computing*, vol. 5, no. 12, pp. 1633–1649, 2006.

[4] M. Kim and D. Kotz, "Periodic properties of user mobility and access-point popularity," *Personal and Ubiquitous Computing*, vol. 11, no. 6, pp. 465–479, 2007.

[5] M. Afanasyev, T. Chen, G.M. Voelker, and A.C. Snoeren, "Analysis of a mixed-use urban WiFi network: when metropolitan becomes neapolitan," *Proc. ACM SIGCOMM Conf. Internet Measurement*, 2008, pp. 85–97.

[6] M. Ylianttila, M. Pande, J. Makela, and P. Mahonen, "Optimization scheme for mobile users performing vertical handoffs between IEEE 802.11 and GPRS/EDGE networks," *Proc. IEEE Global Telecomm. Conf.*, 2001, pp. 3439–3443.

[7] S. Mohanty, "A new architecture for 3G and WLAN integration and inter-system handover management," *Wireless Network*, vol. 12, no. 6, pp. 733–745, 2006.

[8] M. Pischella, F. Lebeugle, and S.B. Jamaa, "UMTS to WLAN handover based on a priori knowledge of the networks," *Proc. IEEE Int'l Conf. Comm.*, vol. 5, 2006, pp. 2009–2013.

[9] F.A. Phiri and M.B. Murthy, "WLAN-GPRS tight coupling based interworking architecture with vertical handoff support," *Wireless Personal Comm.*, vol. 40, no. 2, pp. 137–144, 2007.

[10] P. Yang, H. Deng, and Y. Ma, "Seamless integration of 3G and 802.11 wireless network," *Proc. ACM Int'l Workshop Mobility Management and Wireless Access*, 2007, pp. 60–65.

[11] W. Guan, X. Ling, X. Shen, and D. Zhao, "Handoff trigger table for integrated 3G/WLAN networks," *Proc. ACM Int'l Conf. Wireless Comm. and Mobile Computing*, 2006, pp. 575–580.

[12] R. Prakash and V.V. Veeravalli, "Locally optimal soft handoff algorithm," *Proc. IEEE Vehicular Technology Conf.*, 2000, pp. 1450–1454.

[13] Q.A. Zeng and D.P. Agrawal, "Modeling and efficient handling of handoffs in integrated wireless mobile networks," *IEEE Trans. Vehicular Technology*, vol. 51, no. 6, pp. 1469–1478, 2002.

[14] Q. Zhang, C. Guo, Z. Guo, and W. Zhu, "Efficient mobility management for vertical handoff between WWAN and WLAN," *IEEE Comm. Magazine*, vol. 41, no. 11, pp. 102–108, 2003.

[15] S.K. Kim, C.G. Kang, and K.S. Kim, "An adaptive handover decision algorithm based on the estimating mobility from signal strength measurements," *IEEE Vehicular Technology Conf.*, 2004, pp. 1004–1008.

[16] Y. Wang, P.H. Ho, S. Shen, S. Li, and S. Naik, "Modularized two-step vertical handoff scheme in integrated WWAN and WLAN," *Proc. IEEE Workshop High Performance Switching and Routing*, 2005, pp. 520–524.

[17] O.B. Akan and B. Baykal, "Handoff performance improvement with latency reduction in next generation wireless networks," *Wireless Networks*, vol. 11, no. 3, pp. 319–332, 2005.

[18] M. Ylianttila, J. Makela, and K. Pahlavan, "Analysis of handoff in a location-aware vertical multi-access network," *Computer Networks*, vol. 47, no. 2, pp. 185–201, 2005.

[19] V.P. Kafle, E. Kamioka, and S. Yamada, "A scheme for graceful vertical handover in heterogeneous overlay networks," *Proc. IEEE Int'l Conf. Wireless and Mobile Computing, Networking and Comm.*, 2006, pp. 343–348.

[20] K. Sethom, H. Afifi, and G. Pujolle, "A distributed and secured architecture to enhance smooth handoffs in wide area wireless IP infrastructures," *Mobile Computing and Comm. Review*, vol. 10, no. 3, pp. 46–57, 2006.

[21] R.C. Chalmers, G. Krishnamurthi, and K. C. Almeroth, "Enabling intelligent handovers in heterogeneous wireless networks," *Mobile Networks and Applications*, vol. 11, no. 2, pp. 215–227, 2006.

[22] A.H. Zahran, B. Liang, and A. Saleh, "Signal threshold adaptation for vertical handoff in heterogeneous wireless networks," *Mobile Network Application*, vol. 11, no. 4, pp. 625–640, 2006.

[23] B.J. Chang, S.Y. Lin, and Y.H. Liang, "Minimizing roaming overheads for vertical handoff in heterogeneous wireless mobile networks," *Proc. ACM Int'l Conf. Wireless Comm. and Mobile Computing*, 2006, pp. 957–962.

[24] J. Nie, J. Wen, Q. Dong, and Z. Zhou, "A seamless handoff in IEEE 802.16a and IEEE 802.11n hybrid networks," *Proc. IEEE Int'l Conf. Comm., Circuits and Systems*, 2005, pp. 383–387.

[25] J. Nie, L. Zeng, and J. Wen, "A bandwidth based adaptive fuzzy logic handoff in IEEE 802.16 and IEEE 802.11 hybrid networks," *Proc. IEEE Int'l Conf. Convergence Information Technology*, 2007, pp. 24–29.

[26] A. Garg and K.C. Yow, "Determining the best network to handover among various IEEE 802.11 and IEEE 802.16 networks by a mobile device," *Proc. IEEE Int'l Conf. Mobile Technology, Applications and Systems*, 2005.

[27] Y.C. Jung, B.K. Kim, and Y.T. Kim, "SIP based end-to-end QoS negotiation scheme for MIH," *Proc. IEEE/IFIP Int'l Workshop Broadband Convergence Networks*, 2007.

[28] A.B. Pontes, D.D.P. Silva, J. Jailton, O. Rodrigues, and K.L. Dias, "Handover management in integrated WLAN and mobile WiMAX networks," *IEEE Wireless Comm.*, vol. 15, no. 5, pp. 86–95, 2008.

[29] J.S. Wu, S.F. Yang, and B.J. Hwang, "A terminal-controlled vertical handover decision scheme in IEEE 802.21-enabled heterogeneous wireless networks," *Int'l J. Comm. Systems*, vol. 22, no. 7, pp. 819–834, 2009.

[30] M. Ibrahim, K. Khawam, A.E. Samhat, and S. Tohme, "Analytical framework for dimensioning hierarchical WiMAX-WiFi networks," *Computer Networks*, vol. 53, no. 3, pp. 299–309, 2009.

[31] Y. Choi and S. Choi, "Service charge and energy-aware vertical handoff in integrated IEEE 802.16e/802.11 networks," *Proc. IEEE INFOCOM*, 2007, pp. 589–597.

[32] Y.C. Chen, J.H. Hsia, and Y.J. Liao, "Advanced seamless vertical handoff architecture for WiMAX and WiFi heterogeneous networks with QoS guarantees," *Computer Comm.*, vol. 32, no. 2, pp. 281–293, 2009.

[33] H.T. Lin, Y.Y. Lin, W.R. Chang, and R.S. Cheng, "An integrated WiMAX/WiFi architecture with QoS consistency over broadband wireless networks," *Proc. IEEE Consumer Comm. and Networking Conf.*, 2009, pp. 1–7.

[34] J. Nie, X. He, Z. Zhou, and C. Zhao, "Communication with bandwidth optimization in IEEE 802.16 and IEEE 802.11 hybrid networks," *Proc. IEEE Int'l Symp. Comm. and Information Technology*, 2005, pp. 26–29.

[35] S.F. Yang and J.S. Wu, "Handoff management schemes across hybrid WiMAX and WiFi networks," *Proc. IEEE TENCON*, 2007.

[36] IEEE 802.16 modules on NS-2 of NIST. [Online]. Available: http://www.antd.nist.gov/seamlessandsecure/download.html

[37] BonnMotion: A mobility scenario generation and analysis tool by University of Bonn. [Online]. Available: http://web.informatik.uni-bonn.de/IV/Mitarbeiter/dewaal/BonnMotion/